Fabrication of large-area and low mass critical-angle x-ray transmission gratings

Ralf K. Heilmann, Alex R. Bruccoleri, Dong Guan, and Mark L. Schattenburg,

Space Nanotechnology Laboratory, MIT Kavli Institute for Astrophysics and Space Research, Massachusetts Institute of Technology, Cambridge, Massachusetts 02139, USA

ABSTRACT

Soft x-ray spectroscopy of celestial sources with high resolving power $R = E/\Delta E$ and large collecting area addresses important science listed in the Astro2010 Decadal Survey New Worlds New Horizons, such as the growth of the large scale structure of the universe and its interaction with active galactic nuclei, the kinematics of galactic outflows, as well as coronal emission from stars and other topics. Numerous studies have shown that a transmission grating spectrometer based on lightweight critical-angle transmission (CAT) gratings can deliver R = 3000-5000 and large collecting area with high efficiency and minimal resource requirements, providing spectroscopic figures of merit at least an order of magnitude better than grating spectrometers on Chandra and XMM-Newton, as well as future calorimeter-based missions. The recently developed CAT gratings combine the advantages of transmission gratings (low mass, relaxed figure and alignment tolerances) and blazed reflection gratings (high broad band diffraction efficiency, utilization of higher diffraction orders). Their working principle based on blazing through reflection off the smooth, ultra-high aspect ratio grating bar sidewalls has previously been demonstrated on small samples with x rays. For larger gratings (area greater than 1 inch square) we developed a fabrication process for grating membranes with a hierarchy of integrated low-obscuration supports. The fabrication involves a combination of advanced lithography and highly anisotropic dry and wet etching techniques. We report on the latest fabrication results of free-standing, large-area CAT gratings with polished sidewalls and preliminary x-ray tests.

Keywords: x-ray optics, critical-angle transmission grating, x-ray spectroscopy, blazed transmission grating, soft x-ray, silicon-on-insulator, deep reactive-ion etching

1. INTRODUCTION

The characteristic lines of ionized carbon, nitrogen, oxygen, neon and iron all lie in the soft x-ray band and are central to studies of the Warm Hot Intergalactic Medium, the search for the missing baryons, the study of the outflows of supermassive black holes and the properties of galaxy halos. They can teach us about the evolution of large scale structure and cosmic feedback. In addition, soft x-ray spectroscopy of individual stars can help to reveal the effects of rotation, magnetic fields and stellar winds in stellar coronae. For further details and additional science cases the reader can consult Bautz *et al.*[1] and references therein.

Many of these topics were identified as high-priority science questions in the Astro2010 Decadal Survey "New Worlds New Horizons" (NWNH).[2] To attack a number of these questions requires a soft x-ray grating spectrometer that needs to exceed the capabilities of the HETGS[3] on Chandra and the RGS[4] on XMM-Newton by an order of magnitude or more. Typical performance goals are large collecting area ($>$ 1000 cm^2) and high resolving power ($R = \lambda/\Delta\lambda > 3000$) for point sources. In recent years the x-ray astronomy community has produced an impressive number of mission concepts for a soft x-ray spectrometer, either as a dedicated spectroscopy mission,[1,5–8] or as an instrument on board a larger x-ray observatory.[7,9–13]

X-ray grating spectrometer dispersion provides much larger resolving power for soft x rays ($<\sim$ 2 keV) than imaging microcalorimeters, which have superior resolution $E/\Delta E$ for harder x rays. X-ray gratings come in two main flavors: Reflection[4,11,14,15] and transmission gratings.[3,10,16] Transmission gratings are very thin and offer a mass advantage, especially for large aperture x-ray telescopes. They are also relatively tolerant towards

Further author information: Send correspondence to R.K.H. E-mail: ralf@space.mit.edu, URL: http://snl.mit.edu/home/ralf

Space Telescopes and Instrumentation 2014: Ultraviolet to Gamma Ray, edited by Tadayuki Takahashi, Jan-Willem A. den Herder, Mark Bautz, Proc. of SPIE Vol. 9144, 91441A · © 2014 SPIE
CCC code: 0277-786X/14/$18 · doi: 10.1117/12.2056829

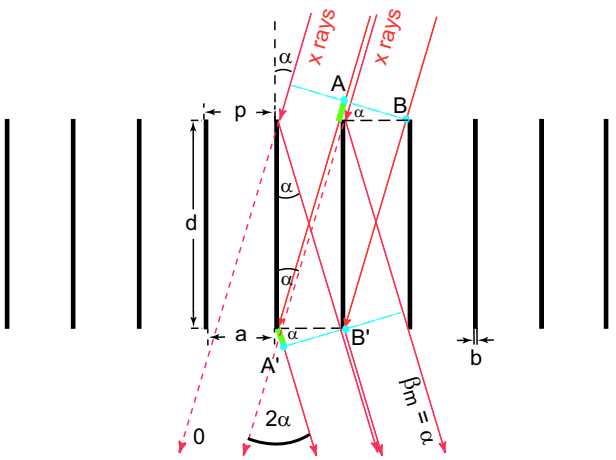

Figure 1. Schematic cross section through a CAT grating of period p. The m^{th} diffraction order occurs at an angle β_m where the path length difference between AA' and BB' is $m\lambda$. Shown is the case where β_m coincides with the direction of specular reflection from the grating bar side walls ($\beta_m = \alpha$), i.e., blazing in the m^{th}order.

misalignment and figure errors, and due to their thinness can be very transparent for hard x rays. (The latter property offers the opportunity to pair an objective transmission grating spectrometer with a microcalorimeter at the telescope imaging focus for simultaneous high-spectral resolution spectroscopy over at least two orders of magnitude in wavelength.[7,9,12,13] This is an opportunity that should not be overlooked in the context of the proposed future ESA L2 mission Athena.[17]) Due to their low mass and thinness they typically do not require additional power for temperature control beyond what is already necessary for telescope mirrors.[10] Traditional phase shifting transmission gratings can only be designed for high diffraction efficiency over a relatively narrow band and for higher x-ray energies.[3] Efficient blazing towards higher diffraction orders - which increases dispersion and therefore spectral resolving power - also would have been impossible with previous transmission grating designs.

The design for critical-angle transmission (CAT) gratings removes these shortcomings, but maintains all the traditional advantages of transmission gratings.

In the following we briefly describe the CAT grating principle. We then present our progress in fabrication and infrastructure over the last year and discuss our future plans.

2. CAT GRATING PRINCIPLE

Critical-angle transmission (CAT) gratings are free-standing transmission gratings with ultra-high aspect-ratio grating bars. They can be described as blazed transmission gratings and combine the advantages of past-generation transmission and blazed reflection gratings.[16,18–20] The basic structure of a CAT grating is shown in Fig. 1 in cross section. X rays are incident onto the nm-smooth side walls of thin, ultra-high aspect-ratio grating bars at an angle α below the critical angle for total external reflection, θ_c (e.g. $\theta_c = 1.7°$ for 1 keV photons reflecting off a silicon surface). For optimum efficiency the grating depth $d = a/\tan\alpha$, (a being the spacing between two adjacent grating bars) the grating bar thickness b should be as small as possible, and the gratings should be free-standing.

We have previously fabricated small CAT grating prototypes with periods of 574[19–21] and 200 nm[10,16,20,22,23] with anisotropic wet etching of lithographically patterned <110> silicon-on-insulator (SOI) wafers in potassium hydroxide (KOH) solutions. We have achieved small grating bar duty cycles ($b/p < 20\%$), unprecedented grating bar aspect ratios (d/b up to 150), and smooth side walls. X-ray tests have shown that our grating prototypes perform at the level of 50-100% of theoretical predictions for ideal CAT gratings over a broad wavelength band.[16,19]

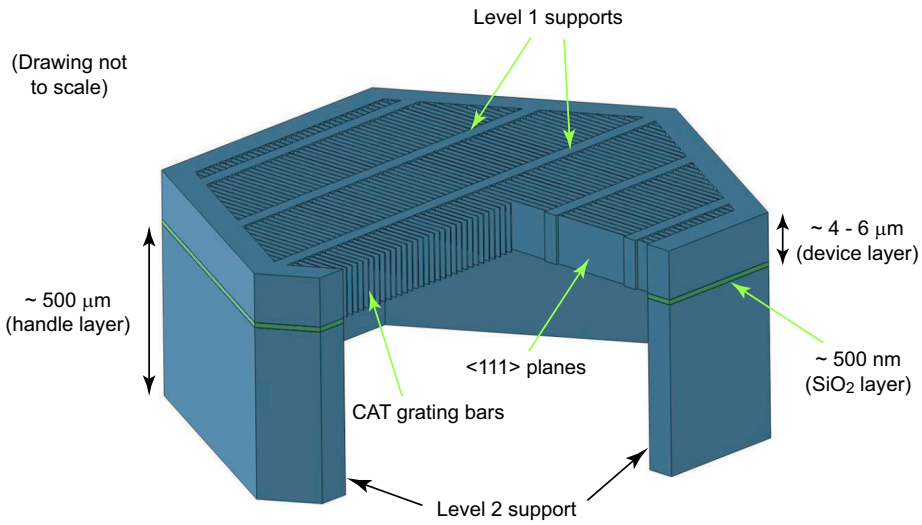

Figure 2. Schematic of a grating membrane "unit cell" (not to scale), formed by a single L2 support mesh hexagon. The L2 mesh is etched out of the SOI handle layer (back side). The device layer contains the fine-period CAT grating bars and in the perpendicular direction the coarse, low duty cycle integrated L1 support mesh. Device and handle layers are separated by the thin buried silicon oxide layer that serves as an etch stop for both front and back side etches.

3. LARGE-AREA CAT GRATINGS

Future space-based soft x-ray spectrographs require grating arrays to span areas on the order of 5,000 cm^2 or more. This is best achieved by tiling the area with reasonably sized grating facets that can be fabricated with standard semiconductor equipment.[10,24] Taking cost and optical design into account, grating facets should be roughly between 30×30 mm^2 and 60×60 mm^2 in size. Grating facets consist of a thin machined frame that can be mounted to a large Grating Array Structure. The frame supports a thin membrane made from a <110> silicon-on-insulator (SOI) wafer. The ∼ 0.5 mm thin handle layer (back side) of the SOI wafer is machined into a high-throughput honeycomb mesh with cell sizes on the order of one to a few mm using Deep Reactive-Ion Etching (DRIE). This so-called Level 2 or L2 mesh provides the necessary stiffness and strength to the membrane. The SOI device layer (front side) is only as thick as the design depth of the CAT grating bars (∼ 4 to 6 μm). It has the grating bars and a Level 1 (L1) cross support mesh (grating with ∼ 5 to 20 μm period) simultaneously etched into it via DRIE. The buried oxide (BOX) layer that separates device and handle layer and serves as an etch stop is removed from the open areas at the end. This creates a free-standing grating structure with two integrated levels of support as part of the membrane (see Fig. 2).

We have fabricated CAT grating membranes in the past that span 31×31 mm^2 with L1 and L2 supports that combined block less than 40% of the grating area.[25,26] See also the right side of Fig. 3.

4. CAT GRATING MEMBRANE FABRICATION

4.1 Overview

The starting point for CAT grating membrane fabrication are SOI wafers. The buried oxide layer serves as an excellent stop for the etching of silicon from the front (device layer) side and the back (handle layer) side. This makes it possible to lithographically define different sets of patterns on the front and back, and for the front and back sides to differ in thickness. We assign the thick back side the task of providing structural strength to a large-area membrane with minimal x-ray blockage. The thin front side contains the CAT grating bars and the integrated L1 support mesh. The key to CAT grating membrane fabrication is to find a sequence of steps that will etch thin ultra-high aspect ratio structures with large open areas uniformly into one side at a time, without compromising the previously etched structures on the other side. In addition, the grating bar sidewalls must be smooth at the 1 nm level or better.[28]

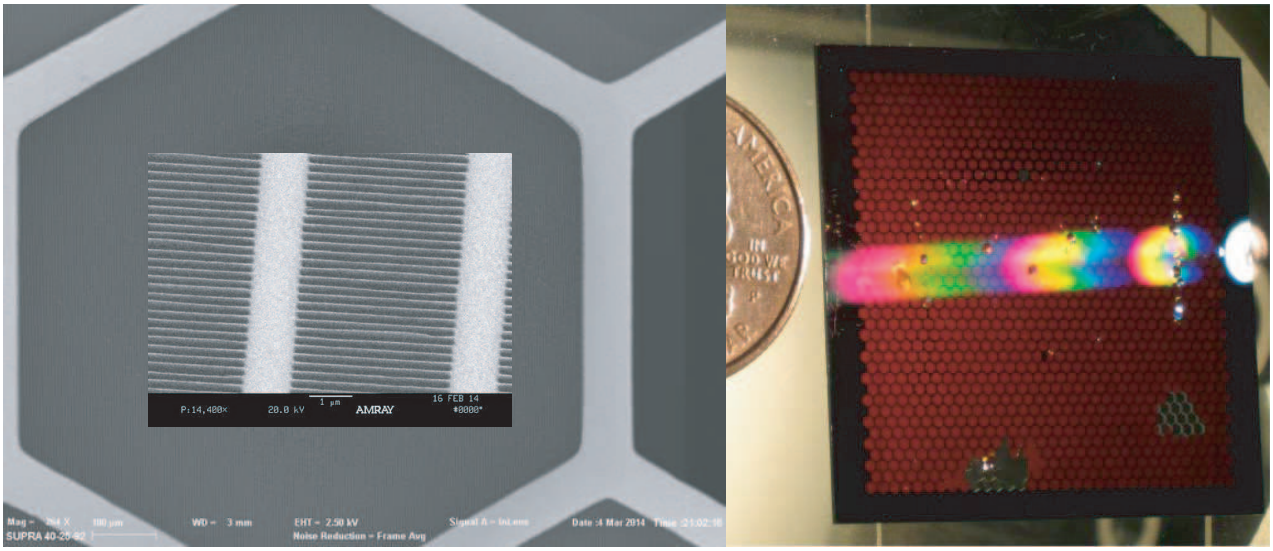

Figure 3. Large CAT grating membrane. Left: Scanning electron micrograph (SEM) of the back side of a grating membrane. The hexagon period is ~ 1 mm, and the L2 mesh lines are ~ 100 μm wide. The insert shows a small area of the membrane back side at larger magnification with L1 supports clearly visible. The much finer CAT grating bars are held in place by the L1 supports. These samples were etched with the combined DRIE/KOH process (see text). Right: Grating membrane next to a U.S. quarter coin. Diffraction is due to the L1 support mesh. The hexagonal L2 mesh is visible due to back illumination. Most membrane defects were caused by intentional tearing for cross-sectional SEM studies. (This sample did not include a KOH etch.)

Our initial goal was to demonstrate the CAT grating principle with x-ray tests on a physical prototype. We fabricated several prototypes using a wet ech in KOH solution, followed by critical-point drying.[21,22] These prototypes were so small in area that they did not require a L2 support mesh. The etch rate of crystalline silicon in KOH differs strongly between different crystal planes. Using interference lithography, we aligned the CAT grating mask pattern on a <110> SOI wafer parallel to the {111} planes that run normal to the wafer surface. With the {111} planes etching over a hundered times slower than other planes we obtained ultra-high aspect-ratio vertical sheets of silicon with nm-smooth {111} planes as sidewalls. These structures performed as CAT gratings in the soft x-ray band in good agreement with theoretical predictions. However, the L1 support bar mask prevents a set of inclined {111} planes from being etched, such that the L1 bars widen substantially with increasing etch depths, and rob much of the open grating area.[16]

Highly anisotropic etching of silicon independent of crystal orientation in principle can also be achieved with deep reactive-ion etching (DRIE), but generally has been done for much larger critical dimensions on the order of several to tens of microns, rather than hundreds or tens of nanometers necessary for the fabrication of CAT gratings with 200 nm period. Over the last 2-3 years we developed masks, pattern transfer and etch recipes for the simultaneous vertical etching of CAT gratings and L1 supports, as well as for the L2 support mesh, first on bulk silicon and separate SOI wafers, and then combined on a single SOI wafer.[24–27] Thus DRIE on the front and back sides of SOI wafers can be used to fabricate large-area, freestanding CAT grating membranes with minimal support structures.

The known main disadvantage of DRIE is that it leaves the CAT grating bar sidewalls too rough, with the best achievable rms roughness on the order of 5 nm or more. We therefore set out to develop a process where DRIE of CAT gratings is followed by a short "polish" in KOH solution. This again requires highly precise alignment of the side walls to the silicon {111} planes during lithography and pattern transfer.[28,29] Not surprisingly, this also puts high demands on the control of process parameters for most fabrication steps. A key question is when to apply the KOH etch. We DRIE the front side first, since the unetched handle layer provides a solid and stable base with homogeneous heat conductivity during the delicate front side DRIE. We then fill the front side grating with resist for protection, and bond the front side to a carrier wafer for the backside DRIE of the L2 mesh. After

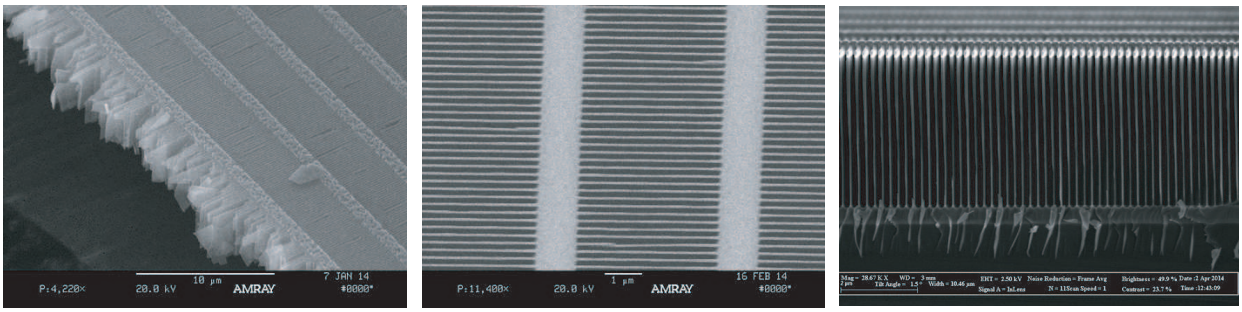

Figure 4. Scanning electron micrographs of 200 nm-period CAT gratings after DRIE and etching in KOH. Left: Torn freestanding membrane, showing L1 supports and CAT grating bars. A few broken grating bars are visible between the L1 supports. Middle: Zoomed in top down view onto front side of freestanding membrane. Right: Cleaved cross section of CAT gratings after frontside DRIE and KOH "polish", and after the new filling process and resist removal. No observable damage, even for very thin ($\sim$ 30 nm) grating lines.

the backside etch we clean the front side and remove the BOX layer in the open areas with a wet HF etch. Filling and cleaning the front side provides a lot of opportunity for damage to the CAT grating bars. The thinner they are, the more easily they get damaged. If we perform the KOH etch before backside DRIE the bars might get too thin. If we perform it afterwards, temporary mechanical deformations during filling and cleaning might lead to faults in the crystal lattice that make the grating bars susceptible to quick destruction in the KOH bath. Ideally we want to "polish" the sidewalls first, then DRIE the back, and then thin the smooth-walled grating bars further without roughening them again.

4.2 Recent Results and Experiments

Despite the above challenges we have succeeded in fabricating the first freestanding, large-area x-ray testable CAT grating membranes with the combined DRIE/KOH process (see left of Fig. 3 and Fig. 4). Unfortunately there are still too many areas with mechanical damage (broken grating bars, rather than bars that are stuck to each other). We believe that the damage is due to the KOH-etched grating bars being too thin to withstand filling and cleaning, as outlined above. On the other hand, preliminary x-ray tests have shown for the first time that CAT gratings that were fabricated with a combined DRIE/KOH process have the required structure and smoothness for efficient blazing in high orders (see left panel in Fig. 5).

We are attacking the issues above with new approaches from multiple sides. First, we have developed a new filling process that is much gentler than the previous one. Instead of just spinning on resist and letting it wick into the space between grating bars, we immerse the grating in a resist solvent and gradually increase the resist concentration until the mixture becomes quite viscous. After cleaning out the resist in the usual manner we do not find any damage, even for grating bars as thin as 30 nm after DRIE/KOH (see Fig. 4). Second, we are investigating a procedure that could enable us to KOH "polish" thick grating bars for a short time before filling, and thin them after removal of the frontside protection without increasing sidewall roughness. Thinning could be achieved through repeated thermal oxidation, followed by oxide removal in HF vapor. During thermal oxidation the interface between oxide and silicon moves into the silicon, such that less silicon remains after the thick oxide is removed. For initial results see Fig. 5. This process can be done "dry", i.e. without complications due to surface tension induced stiction or other mechanical forces during wet etching. We are currently devising experiments to test the roughness of surfaces similar to the grating bar sidewalls after KOH etching and repeated oxidation/vapor HF etch.

Another potentially yield-improving step is the replacement of traditionally compressively stressed BOX layers that tend to buckle with our newly designed tetraethoxysilane layers that can be made with slightly tensile stress and still work well as DRIE etch stops.[30,31]

4.3 Acquisition of a dedicated DRIE tool

Until very recently we had to perform all of our DRIE steps remotely in a shared tool in an open user facility at the University of Michigan. At least two DRIE steps had to be performed per sample, with intermediate processing to

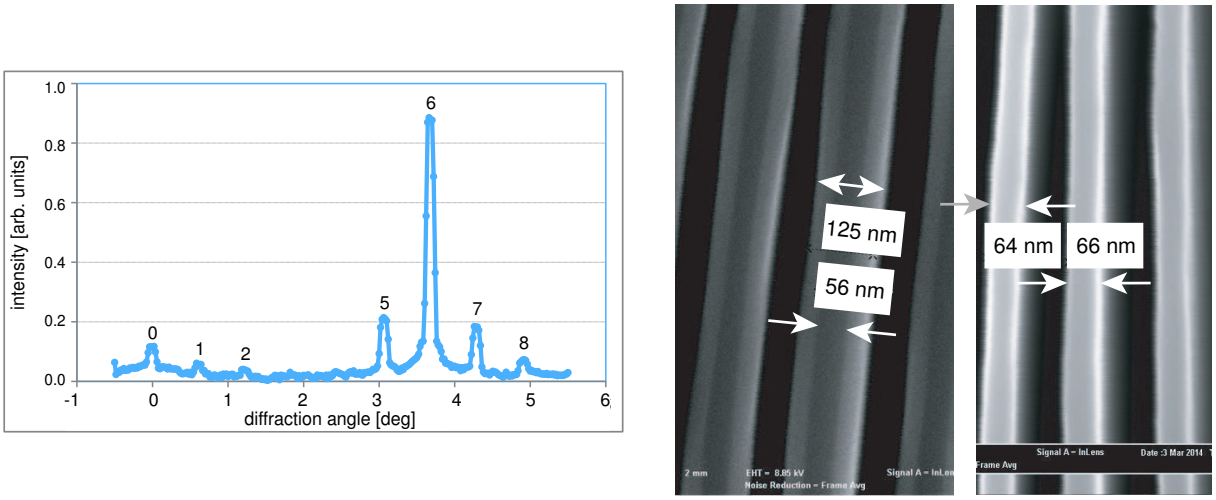

Figure 5. Left: Measured transmission diffraction peaks of a DRIE'd and KOH "polished" 200 nm-period CAT grating for 2.2 nm-wavelength x rays blazed in 6^{th} order. (The 6^{th} order provides six times the resolving power of the 1^{st} order.) Middle: SEM of a cleaved cross section of CAT grating bars after thermal oxidation, clearly showing the thick oxide layers covering the thinned silicon grating bars. The original silicon bar thickness was $\sim$ 110 nm. Right: SEM of silicon grating bars after oxide removal.

be done at MIT. This logisitcal complication was very time consuming and slowed down our process development. Over the last year we worked on the selection, acquisition, infrastructure preparation, installation, testing and qualification of a dedicated advanced DRIE tool at the Space Nanotechnology Laboratory at MIT. Selection entailed the production of a large number of patterned and masked samples to send to several commercial DRIE tool vendors for front and back side etch demonstrations. We selected one of the candidate tools after several rounds of samples and careful evaluations and analysis of the etch results. The tool is now finally being used to repeat results from the work done at Michigan and to continue process development from there.

5. FUTURE PLANS

Our near-term plan is to produce higher-quality large-area CAT grating membranes and to verify grating performance through diffraction efficiency measurements. We will then demonstrate CAT grating resolving power in an x-ray imaging system. For example we can use Technology Development Module optics from Zhang *et al.*[32] in the Marshall Space Flight Center Stray Light Test Facility as an imaging system.[33] However, demonstrating $R = 3000$ at this facility has only recently become possible using very high diffraction orders and many hours of integration time for a single diffraction peak. It is far from trivial to find or construct a facility that has better capabilities today. The dominant limiting factor in achieving $R = 3000$ for a CAT grating spectrometer is the variation in grating period. As an alternative, instead of demonstrating resolving power in an imaging system we can directly measure the CAT grating period over the whole area of a grating facet with high enough precision with a technique similar to quality control measurements on the transmission gratings for Chandra.[34]

The optical design of a CAT grating spectrometer is well understood,[6,10] and the alignment and grating flatness requirements are within present day standard technology and engineering capabilities. Nevertheless, in order to increase Technology Readiness Level from the current 3 to 4 and 5 it will be necessary to demonstrate high-quality grating facets (membranes fabricated from SOI wafers and mounted to a frame) and to build a brass board grating array that is populated with several high-quality, large-area grating facets, and for the array to pass repeated x-ray and environmental testing. With appropriate funding, manpower and facilities access we can reach TRL5 by the end of 2016 and TRL6 by the end of 2018. More details can be found in the NASA Technology Development Roadmap for a near-term probe-class X-ray astrophysics mission[35] and annual Physics of the Cosmos Program Annual Technology Reports.[36]

6. SUMMARY

A large-area grating spectrometer is the only choice for greatly improved high-resolution studies of astrophysical sources in the soft x-ray band feasible for launch within this decade. X-ray astronomy would gain the most from a mission that combines a microcalorimeter at the focus of a large-collecting-area telescope with a CAT grating spectrometer. The CAT grating principle has been demonstrated experimentally, and we are proceeding with the fabrication development and testing of large-area CAT gratings. Our technology development is on schedule, and with appropriate funding we can achieve TRL5 by the end of 2016 and in time for a potential explorer x-ray mission start as early as 2017.

ACKNOWLEDGMENTS

We gratefully acknowledge technical support from F. DiPiazza (Silicon Resources) and facilities support from the Nanostructures Laboratory and the Microsystems Technology Laboratories (both at MIT). This work was performed in part at the Lurie Nanofabrication Facility, a member of the National Nanotechnology Infrastructure Network, which is supported by the National Science Foundation, and at the Advanced Light Source at Lawrence Berkeley National Lab, which is supported by the Director, Office of Science, Office of Basic Energy Sciences, of the U.S. Department of Energy under Contract No. DE-AC02-05CH11231. This work was supported by NASA grants NNX11AF30G and NNX12AF21G.

REFERENCES

[1] M. W. Bautz *et al.*, "AEGIS - an astrophysics experiment for grating and imaging spectroscopy," Response to NASA solicitation NNH11ZDA018L, http://pcos.gsfc.nasa.gov/studies/rfi/Bautz-Marshall-RFINNH11ZDA018L.pdf (2011).

[2] "New Worlds, New Horizons in Astronomy and Astrophysics," National Research Council, http://www.nap.edu/catalog.php?record_id=12951 (2010).

[3] C. R. Canizares *et al.*, "The Chandra high-energy transmission grating: Design, fabrication, ground calibration, and 5 years in flight," *PASP* **117**, 1144-1171 (2005).

[4] J. W. den Herder *et al.*, "The reflection grating spectrometer on board XMM-Newton," *Astr. & Astroph.* **365**, L7-L17 (2001).

[5] M. W. Bautz *et al.*, "Concepts for high-performance soft x-ray grating spectroscopy in a moderate-scale mission," *Proc. SPIE* **8443**, 844315 (2012).

[6] J. E. Davis, M. W. Bautz, D. Dewey, R. K. Heilmann, J. C. Houck, D. P. Huenemoerder, H. L. Marshall, M. A. Nowak, and M. L. Schattenburg, "Raytracing with MARX - X-ray observatory design, calibration, and support," *Proc. SPIE* **8443**, 84431A (2012).

[7] NASA X-ray Mission Concepts Study Project Report, http://pcos.gsfc.nasa.gov/physpag/X-ray_Mission_Concepts_Study_Report-Final.pdf

[8] R. K. Smith *et al.*, "Arcus: An ISS-attached high-resolution x-ray grating spectrometer," these proceedings.

[9] J. Bookbinder, "An overview of the IXO Observatory," *Proc. SPIE* **7732**, 77321B (2010).

[10] R. K. Heilmann *et al.*, "Critical-angle transmission grating spectrometer for high-resolution soft x-ray spectroscopy on the International X-Ray Observatory," *Proc. SPIE* **7732**, 77321J (2010).

[11] R. L. McEntaffer *et al.*, "Development of off-plane gratings for WHIMex and IXO," *Proc. SPIE* **8147**, 81471K (2011).

[12] J. A. Bookbinder *et al.*, "The Advanced X-ray Spectroscopic Imaging Observatory (AXSIO)," *Proc. SPIE* **8443** 844317 (2012).

[13] A. Vikhlinin *et al.*, "SMART-X: Square Meter Arcsecond Resolution X-Ray Telescope," *Proc. SPIE* **8443** 844316 (2012).

[14] C.-H. Chang, J. C. Montoya, M. Akilian, A. Lapsa, R. K. Heilmann, M. L. Schattenburg, M. Li, K. A. Flanagan, A. P. Rasmussen, J. F. Seely, J. M. Laming, B. Kjornrattanawanich, and L. I. Goray, "High fidelity blazed grating replication using nanoimprint lithography," *J. Vac. Sci. Technol. B* **22**, 3260–3264 (2004).

[15] J. F. Seely, L. I. Goray, B. Kjornrattanawanich, J. M. Laming, G. E. Holland, K. A. Flanagan, R. K. Heilmann, C.-H. Chang, M. L. Schattenburg, and A. P. Rasmussen, "Efficiency of a grazing-incidence off-plane grating in the soft-x-ray region," *Appl. Opt.* **45**, 1680–1687 (2006).

[16] R. K. Heilmann, M. Ahn, A. Bruccoleri, C.-H. Chang, E. M. Gullikson, P. Mukherjee, and M. L. Schattenburg, "Diffraction efficiency of 200 nm period critical-angle transmission gratings in the soft x-ray and extreme ultraviolet wavelength bands," *Appl. Opt.* **50**, 1364-1373 (2011).

[17] K. Nandra *et al.*, "Athena: Exploring the hot and energetic universe," these proceedings.

[18] R. K. Heilmann *et al.*, "Critical-angle transmission gratings for high resolution, large area soft x-ray spectroscopy," Response to NASA solicitation NNH11ZDA018L, http://pcos.gsfc.nasa.gov/studies/rfi/Heilmann-Ralf-RFINNH11ZDA018L.pdf (2011).

[19] R. K. Heilmann, M. Ahn, E. M. Gullikson, and M. L. Schattenburg, "Blazed high-efficiency x-ray diffraction via transmission through arrays of nanometer-scale mirrors," *Opt. Express* **16**, 8658-8669 (2008).

[20] R. K. Heilmann, M. Ahn, and M. L. Schattenburg, "Fabrication and performance of blazed transmission gratings for x-ray astronomy," *Proc. SPIE* **7011**, 701106 (2008).

[21] M. Ahn, R. K. Heilmann, and M. L. Schattenburg, "Fabrication of ultrahigh aspect ratio freestanding gratings on silicon-on-insulator wafers," *J. Vac. Sci. Technol. B* **25**, 2593-2597 (2007).

[22] M. Ahn, R. K. Heilmann, and M. L. Schattenburg, "Fabrication of 200 nm-period blazed transmission gratings on silicon-on-insulator wafers," *J. Vac. Sci. Technol. B* **26**, 2179-2182 (2008).

[23] R. K. Heilmann *et al.*, "Development of a critical-angle transmission grating spectrometer for the International X-Ray Observatory," *Proc. SPIE* **7437**, 74370G (2009).

[24] R. K. Heilmann, A. Bruccoleri, P. Mukherjee, J. Yam, and M. L. Schattenburg, "Fabrication update on critical-angle transmission gratings for soft x-ray grating spectrometers," *Proc. SPIE* **8147**, 81471L (2011).

[25] R. K. Heilmann, A. Bruccoleri, P. Mukherjee, and M. L. Schattenburg, "Progress in the Development of Critical-Angle Transmission Gratings," *Proc. SPIE* **8443**, 84430W (2012).

[26] A. Bruccoleri, P. Mukherjee, R. K. Heilmann, J. Yam, and M. L. Schattenburg, "Fabrication of nanoscale, high throughput, high aspect ratio freestanding gratings," *J. Vac. Sci. Technol. B* **30** 06FF03 (2012).

[27] P. Mukherjee, A. Bruccoleri, R. K. Heilmann, M. L. Schattenburg, A. F. Kaplan, and L. J. Guo, "Plasma etch fabrication of 60:1 aspect ratio silicon nanogratings on 200 nm pitch," *J. Vac. Sci. Technol. B* **28**, C6P70-5 (2010).

[28] A. R. Bruccoleri, D. Guan, S. Vargo, F. DiPiazza, R. K. Heilmann, and M. L. Schattenburg, "Nanofabrication advances for high efficiency critical-angle transmission gratings," *Proc. SPIE* **8861**, 886119 (2013).

[29] A. R. Bruccoleri, D. Guan, P. Mukherjee, R. K. Heilmann, M. L. Schattenburg, and S. Vargo, "Potassium hydroxide polishing of nanoscale deep reactive-ion etched ultra-high aspect ratio gratings," *J. Vac. Sci. Technol. B* **31**, 06FF02 (2013).

[30] D. Guan, A. R. Bruccoleri, R. K. Heilmann, and M. L. Schattenburg, "Stress control of plasma enhanced chemical vapor deposited silicon oxide film from tetraethoxysilane (TEOS)," *J. Micromech. Microeng.* **24**, 027001 (2014).

[31] D. Guan, "Fabrication of stress controlled silicon oxide for freestanding MEMS devices," M.S. thesis, Dept. of Mechanical Engineering, Massachusetts Institute of Technology (2014).

[32] W. W. Zhang *et al.*, "Next generation astronomical x-ray optics: high angular resolution, light weight, and low production cost," *Proc. SPIE* **8443**, 84430S (2012).

[33] R. McEntaffer *et al.*, "First results from a next-generation off-plane X-ray diffraction grating," *Exp. Astron.* **36**, 389 (2013).

[34] D. Dewey, D. N. Humphries, G. Y. McLean, and D. A. Moschella, "Laboratory calibration of x-ray transmission diffraction gratings," *Proc. SPIE* **2280**, 257 (1994).

[35] NASA Technology Development Roadmap for a near-term probe-class X-ray astrophysics mission, http://pcos.gsfc.nasa.gov/docs/TDR-Final-Aug2013.pdf (2013).

[36] Program Annual Technology Report, http://pcos.gsfc.nasa.gov/technology/PCOS_PATR_2013.pdf